

THE CONTROL OF BEAM DYNAMICS IN HIGH ENERGY INDUCTION LINACS

George J. Caporaso  
Livermore National Laboratory  
P. O. Box 808, Livermore, California

Abstract

The Advent of laser-ion-guiding in the Advanced Test Accelerator along with the development of accelerator cavities optimized with respect to beam breakup coupling impedance now make it possible to consider a new class of high current, high energy linear induction accelerators. The control of the beam breakup and other instabilities by laser guiding and by various magnetic focusing schemes will be discussed along with the scaling laws for the design of such machines to minimize the growth of the beam breakup instability.

Many linacs, particularly induction linacs are limited in performance by the beam breakup (BBU) instability. The instability is found in two forms.<sup>1</sup> In the first form the accelerating cavities communicate with one another through interaction with the beam and through propagation of cavity fields through the accelerator structure. In the second form which is the more virulent of the two, the cavities couple to each other only through their interactions with the beam. It is this second form of BBU that will be discussed in this paper.

Beam Breakup Model

An extremely useful model of BBU will now be described.<sup>2</sup> The accelerating cavities are treated as continuously distributed along the structure. The BBU cavity mode is characterized by its angular frequency  $\omega_0$ , its Q or quality factor and its  $Z_1/Q$  or transverse shunt impedance. The mode is excited by a dipole current source term which is proportional to the product of the beam's current and transverse displacement. The transverse position of the beam centroid is determined by the external linear focusing and the cavity fields.

The force exerted on the beam by the mode is due to the transverse magnetic field of the mode. We define the quantity  $\Delta$ , the z-averaged transverse angular change of the beam centroid per unit length as  $\Delta = (\Delta p_{\perp}/p_z)/L_g$  where  $L_g$  is the average gap to gap separation and  $\Delta p_{\perp}$  and  $p_z$  are the change in transverse momentum and the longitudinal momentum respectively. With this definition the model equations are

$$(\partial^2/\partial\tau^2 + (\omega_0/Q) \partial/\partial\tau + \omega_0^2) \Delta = \omega_0^2 G\xi/\gamma \quad (1)$$

$$\partial/\partial z [\gamma \partial \xi/\partial z] + \gamma k_{\beta}^2 \xi = \gamma \Delta \quad (2)$$

where  $k_{\beta}$  is the betatron wavenumber due to the applied focusing force. The quantity  $G = \omega_0(Z_1/Q)I/(I_0L_g)$  where  $I_0 = mc^3/e \approx 17$  kA. When the focusing is due to solenoids  $k_{\beta}$  is to be interpreted as one half of the cyclotron wavenumber and the displacement  $\xi$  is equal to the phasor  $x + iy$ . For focusing due to an ion or quadrupole channel  $\xi$  represents either the  $x$  or  $y$  component of transverse beam position.

We may solve these equations by first Fourier transforming in the variable  $\tau$  to  $\omega$ . Transformed quantities are denoted by tildes. We also take the case of constant acceleration such that  $\gamma = \gamma_0 + \lambda z$ . Defining  $\tilde{\Psi} = \tilde{\xi}/\gamma$  and using the W.K.B. approximation we

have

$$\partial^2 \tilde{\Psi}/\partial z^2 + [k_{\beta}^2 - h(\omega)/\gamma] \tilde{\Psi} = 0 \quad (3)$$

with solution

$$\xi = \exp \left[ -1 \int_0^z [k_{\beta}^2 - h(\omega)/\gamma]^{1/2} dz' \right] \quad (4)$$

where  $h(\omega) = \omega_0^2 G/(\omega_0^2 - \omega^2 + i\omega\omega_0/Q)$ . For "sufficiently strong" focusing, i.e. for the case that  $k_{\beta}^2 \gg h(\omega)/\gamma$  we obtain the growth of the instability from the inverse Fourier transform

$$\xi = \int_{-\infty}^{\infty} d\omega \frac{\Lambda(\omega)}{2\pi} \exp \left[ i\omega\tau + ih(\omega)/2 \int_0^z dz'/\gamma k_{\beta} \right] \quad (5)$$

This integral may be evaluated by the method of steepest descents to yield the growth laws:<sup>4</sup>

$$\text{For } k_{\beta} = k_0/\gamma \quad \xi \sim \exp[GQ(\gamma - \gamma_0)/(2k_0\lambda)] \quad (6)$$

$$\text{For } k_{\beta} = k_0/\sqrt{\gamma} \quad \xi \sim \exp[GQ(\sqrt{\gamma} - \sqrt{\gamma_0})/k_0\lambda] \quad (7)$$

$$\text{For } k_{\beta} = k_0 \quad \xi \sim \exp[GQ \ln(\gamma/\gamma_0)/(2k_0\lambda)] \quad (8)$$

Equation (6) is appropriate for the case of a constant strength solenoid or alternating quadrupole channel which agrees with the peak growth rate determined in previous work.<sup>3</sup> Equation (7) is appropriate for a constant strength ion channel or a solenoid or quadrupole channel whose strength increases proportionally to  $\sqrt{\gamma}$ . Equation (8) is appropriate for the case where the strength of the channel increases with energy in such a manner as to maintain a constant betatron wavelength. Since the beam breakup instability is convective in the beam frame the above expressions are correct only if the beam pulse is sufficiently long to contain the maximum of the envelope of the instability. Thus the expressions (6) - (8) are maximum growth rates.

Cavity Mode Model

A useful cavity model that yields the scaling of cavity coupling impedances with cavity dimensions was recently developed.<sup>5</sup> A schematic of the model is shown in Fig. 1. The cavity is treated as a radial line of width  $w$  coupled to an open pipe of radius  $b$ . The connection of the radial line to the external world is modelled as a lumped surface impedance at the outer radius  $R$ . In the absence of the gap a dipole return current would flow in the wall as a result of a displaced beam passing through the pipe. The excitation of cavity fields due to the beam can be conveniently represented by a surface dipole current source in the gap of value equal and opposite to the wall current that would flow in the absence of the gap.

An expression for the z-component of vector potential in the pipe is written down in terms of a Fourier integral. A z-independent expression for the vector potential is taken in the radial line. The wave impedance (azimuthal magnetic field/z-component

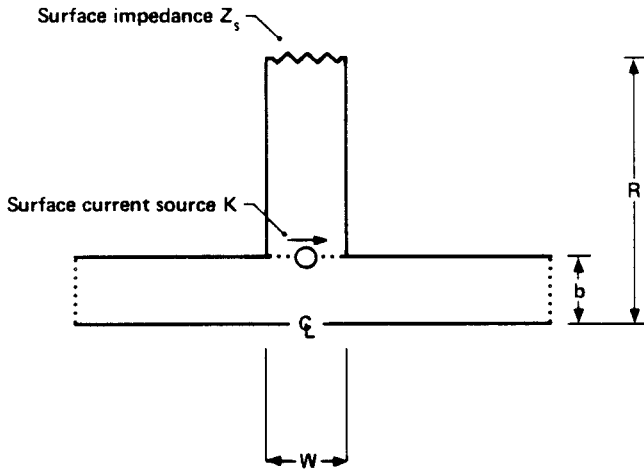


Fig. 1. Schematic of the cavity mode model. The beam excitation is represented as a surface dipole current source in the gap of width  $w$ . The cavity is coupled to an infinitely long pipe of radius  $b$ . The cavity is terminated at radius  $R$  by a lumped surfaced impedance  $Z_s$  which represents the connection to the outside world.

of electric field) is set equal to the surface impedance at  $r = R$  and the  $z$ -averaged jump in azimuthal field across the gap is set equal to  $4\pi K/c$  where  $K$  is the dipole surface current density of the source in the gap. The transverse force on the beam is due to the transverse magnetic field. The Lorentz force is integrated along the path of the beam through the gap. This impulse divided by  $4\pi K/c$  is termed the response function. From the BBU model discussed previously we see that the instability arises from the imaginary part of the cavity response since that part represents the portion of the response that is 90 degrees out of phase with the actual beam displacement. Thus the quantity of interest for BBU is the imaginary part of the response function. The quantity  $\omega_0 Z_1$  may be shown to be equal to  $-4w/b^2$  multiplied by the imaginary part of the response function at the mode frequency  $\omega_0$ . Cold tests of the cavities used in the Advanced Test Accelerator show a  $Q$  of roughly 4 for the dominant BBU mode at 785 MHz. A diagram of the cavity is shown in Fig. 2. Choosing a surface impedance of roughly twice the impedance of free space yields a model response curve with the correct  $Q$  value. The imaginary part of the response function for this case is shown in Fig. 3.

For a given pipe radius and gap width the minimum absolute value of the peak of the imaginary part of the response function occurs when the fields in the radial line are assumed to be purely outgoing. That is, the gap is taken to be perfectly matched to the radial line. This minimum value is a slowly varying function of  $w/b$  and is shown in Fig. 4. The new prototype cavity of the Accelerator Research Center at Livermore is shown in Fig. 5. The shape of the radial line is designed to approximate a perfect match. The imaginary part of the response function for a perfect match is shown in Fig. 6.

#### Laser Ion-Guiding

In laser ion-guiding the accelerator is filled with a very low pressure of an easily ionizable gas (ATA uses benzene at a pressure of  $\approx .2 \mu\text{m}$ ). A small diameter laser beam is then fired down the axis

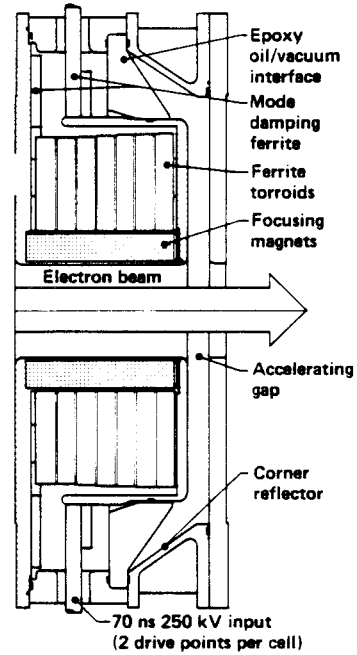
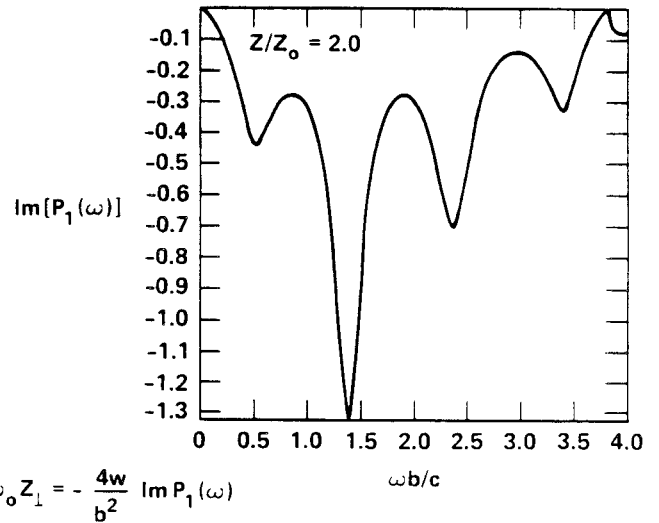


Fig. 2. Diagram of the ATA induction cavity. The cavity has a 2.54 cm gap width and a pipe radius of 6.7 cm. The corner reflector and pieces of damping ferrite lower the  $Q$  of the BBU mode to  $\approx 4$ .



$$\omega_0 Z_1 = -\frac{4w}{b^2} \text{Im} P_1(\omega)$$

Fig. 3. Shown is the imaginary part of the response function for a surface impedance twice that of free space which corresponds to the ATA cell of Fig. 2.

of the machine (ATA employs a .4J KrF laser with a spot diameter of  $\approx 1.5$  cm). A low density plasma channel is then created by photo-ionization of the background gas. When a relativistic electron beam is injected onto the channel the radial electric field of the beam rapidly expels the secondary electrons leaving behind a column of positively charged ions which guide and focus the beam.

From the perspective of controlling beam instabilities ion channel guiding has three important advantages. First, the strength of the channel can be made very strong. Second is the favorable scaling of the betatron wavelength with energy. The betatron

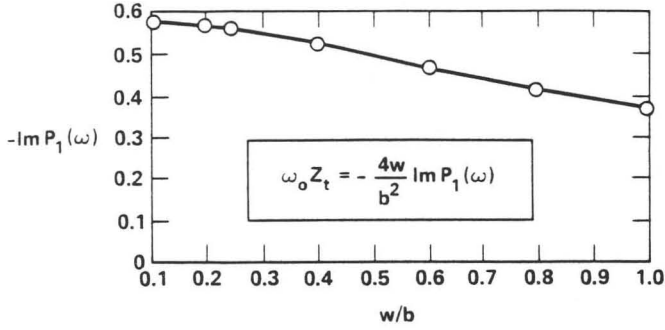


Fig. 4. Plotted is the peak value of the imaginary part of the response function for the case of a perfect match of the gap to the radial line as a function of  $w/b$ .

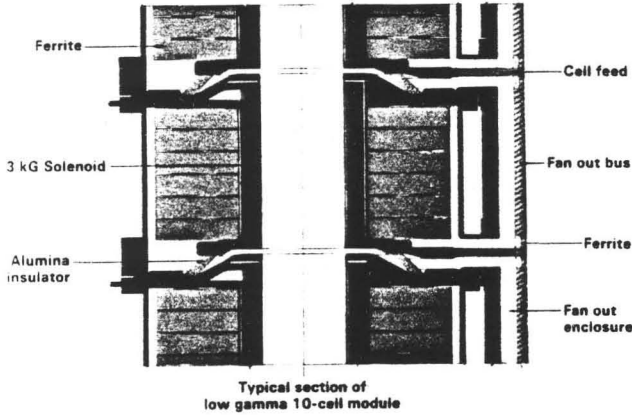
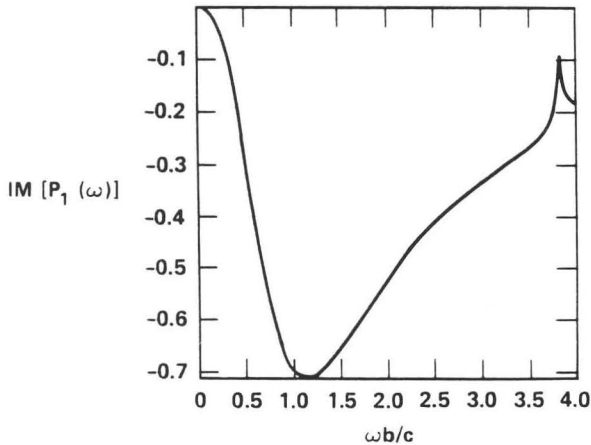


Fig. 5. The prototype cells at the Accelerator Research Center. The radial lines are shaped to approximate a perfect match.



$$\omega_0 Z_{\perp} = -4W/b^2 \text{Im } P_1(\omega)$$

Fig. 6. Shown is the imaginary part of the response function for the gap perfectly matched to the radial line.

wavelength of a solenoid channel or an alternating quadrupole channel increases as  $\gamma$  while the betatron wavelength of the ion channel increases only as  $\sqrt{\gamma}$  leading to tremendous increases in focusing strength (as compared to quadrupole channels) with increasing beam energy. The image displacement instability has a similar scaling with energy so that the use of ion

guiding can be made to suppress this instability at all energies. Thirdly, the electrostatic potential of the ion channel is anharmonic leading to a spread in the betatron wavelength of the beam electrons.

The spread in the betatron wavenumber due to the nonlinear restoring force of the channel has profound implications for the beam breakup instability. Indeed, if the spread in  $k_{\beta}$  is sufficiently great acceleration to arbitrarily high energy is possible without any BBU growth whatever. This result may be derived from an extension of the continuous model presented earlier. We divide the beam into "filaments" each with a different  $k_{\beta}$ . We label the filaments by the variable  $\eta$  and let the corresponding square of the betatron wavenumber be equal to  $\eta k_{\beta}^2$ . We choose a simple distribution for the filaments:<sup>2</sup>

$$g(\eta) = 0 \quad 0 < \eta < 1 - \epsilon$$

$$g(\eta) = 1/\epsilon \quad 1 - \epsilon < \eta < 1$$

where the beam transverse position is now given by an average over the filaments:

$$\xi = \int_0^1 g(\eta) \xi_{\eta} d\eta \quad (9)$$

The model equations now become

$$(\partial^2/\partial\tau^2 + (\omega_0/Q) \partial/\partial\tau + \omega_0^2) \Delta = \omega_0^2 G\xi/\gamma \quad (10)$$

$$\partial/\partial z [\gamma \partial \xi_{\eta} / \partial z] + \gamma \eta k_{\beta}^2 \xi_{\eta} = \gamma \Delta \quad (11)$$

Again we take the case of constant acceleration and define  $\zeta = \gamma\tau$ . We may then Fourier transform in  $\tau$  to  $\omega$  so that Eq. (11) becomes

$$\begin{aligned} \partial^2 \tilde{\xi}_{\eta} / \partial \zeta^2 + 1/\zeta \partial \tilde{\xi}_{\eta} / \partial \zeta + 4\eta k_0^2 \tilde{\xi}_{\eta} / \lambda^2 \\ = 4h(\omega) / (\lambda^2 \epsilon) \int_{1-\epsilon}^1 d\eta \tilde{\xi}_{\eta} \end{aligned} \quad (12)$$

We let  $\tilde{\xi}_{\eta} = \int_0^{\infty} A_{\eta}(k, \omega) J_0(k\zeta) dk$  and substitute into Eq. (12) to obtain

$$A_{\eta}(k, \omega) = 4h(\omega) / (\lambda^2 \epsilon [4\eta k_0^2 / \lambda^2 - k^2]) \int_{1-\epsilon}^1 A_{\eta}(k, \omega) d\eta$$

Application of Eq. (9) to this expression yields the dispersion relation

$$k^2 = 4k_0^2 / \lambda^2$$

$$\pi[(1 - \epsilon) \exp(\epsilon k_0^2 / h(\omega)) - 1] / [\exp(\epsilon k_0^2 / h(\omega)) - 1] \quad (13)$$

Analysis of this relation reveals that for a sufficiently large value of  $\epsilon$  no growth at all occurs.<sup>4</sup> The condition for zero growth is

$$\epsilon k_0^2 > \pi(\omega_0 Z_{\perp} / L_g) (I/I_0) \quad (14)$$

Since  $k_0^2 \approx 2e\hat{\lambda}/(mc^2 a^2)$  where  $a$  is the channel radius and  $\hat{\lambda}$  is the total channel charge per unit length we may rewrite this condition as

$$2\hat{\lambda}\epsilon/a^2 > \pi I \omega_0 Z_{\perp} / L_g \quad (15)$$

ATA Operational Experience

The ATA is a 50 MeV, 10 kA electron induction linac located at Lawrence Livermore National Laboratory's Site 300. The accelerator consists of a 2.5 MeV injector and 174 cavities grouped into 1 block of 9 cells, 5 blocks of 5 cells and 14 blocks of 10 cells. Each cell provides a nominal accelerating voltage of 250 kV. During conventional operation the accelerator focusing is provided by approximately 250, 3 kilogauss capacity solenoids which are closely spaced along the entire machine. Coils are included inside the accelerating cavities in order to approximate a continuous solenoid throughout ATA.

When using laser ion-guiding the beam is magnetically guided from the injector through the first several accelerator cell blocks onto the ion channel. The laser is fired through a hole in the center of the cathode. A diagram showing the pressure and magnetic field profiles for ATA under the two different types of transport is shown in Fig. 7.

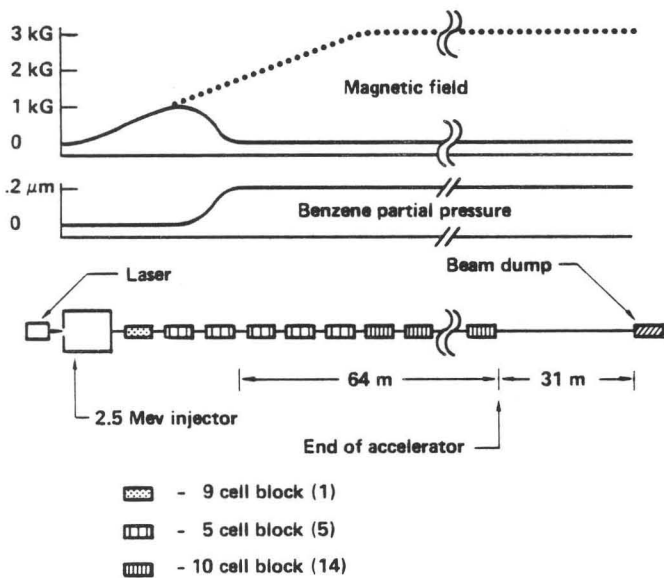


Fig. 7. Illustration of the two transport modes in ATA. Under solenoidal guiding the magnetic field ramps up from zero at the cathode to its maximum value of 3 kG where it is maintained throughout the rest of the accelerator. When using laser guiding the machine is filled with benzene from the low energy end of the machine throughout the accelerator. The magnetic field is used to guide the beam from the injector onto the channel. Beyond this "match point" the magnets are shut off.

Magnetic transport of high beam currents is not possible in ATA because of BBU. The component of transverse displacement at the 785 MHz BBU frequency was measured at the output of the injector to be approximately  $2 \times 10^{-4}$  cm. Using this value and Eq. (6) the expected BBU amplitude at the end of the machine is shown in Fig. 8. Figure 9 shows the results of an attempt to propagate a 7 kA beam. BBU grows to such an extent that only half of the beam charge is transported to the end of the accelerator.

In contrast, Fig. 10 shows the results for laser guiding of a 10 kA beam. The entire pulse is transported and the final BBU amplitude is equal to or less than 0.01 cm. In operation of ATA the benzene pressure is typically set at  $\approx 2 \times 10^{-4}$

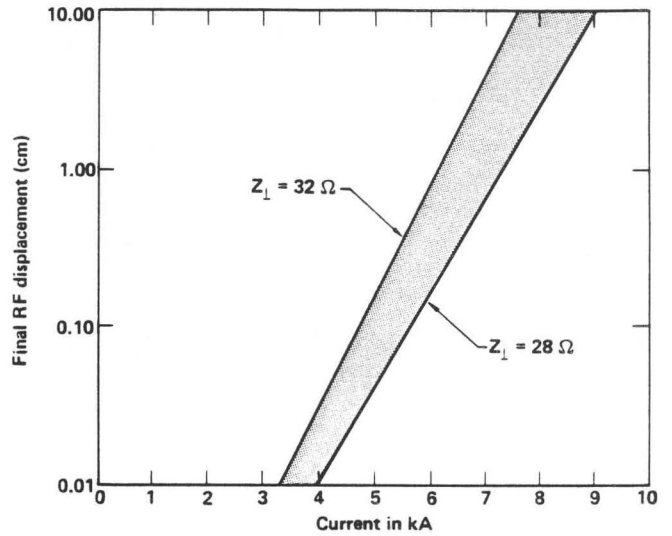


Fig. 8. Final value of the BBU amplitude at the end of ATA versus beam current. The curve is obtained using Eq. (6) and the measured noise output of the injector and cavity parameters.

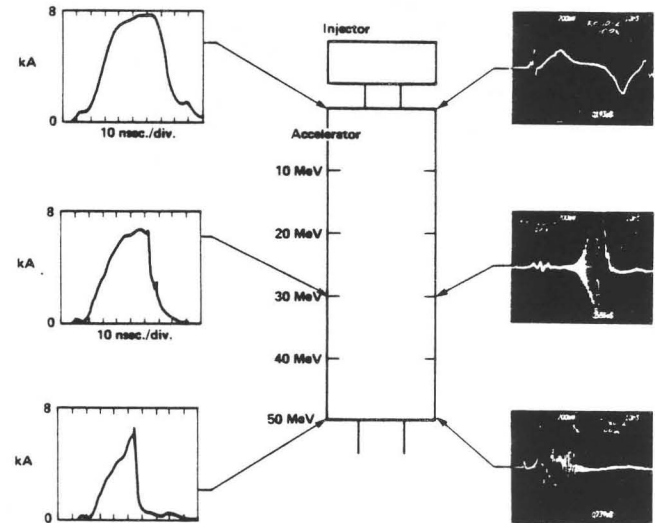


Fig. 9. Propagation of a 7 kA pulse through ATA under solenoidal guiding. The beam current at left shows a steady erosion of the tail of the pulse. Only half of the original charge survives passage through the accelerator. Shown on the right are  $B_0$  loop signals which show the 785 MHz BBU signals. The amplitude of the signals grows down the machine until the downstream end where the beam is hitting the pipe wall shorting the loops out.

torr. The KrF laser produces a nominal .4J, 27 ns FWHM pulse in a spot size about 1.5 cm in diameter. Solutions of a multilevel rate equation model suggest that the benzene is approximately 1% ionized so that the ion density is  $\approx 8.4 \times 10^{11} \text{ cm}^{-3}$  yielding a channel charge of  $\approx 67 \text{ esu/cm}$  and a betatron wavelength of  $\approx 17\sqrt{\gamma}(\text{cm})$ .<sup>6</sup> Betatron wavelengths down to  $\approx 1$  meter have been measured at the output of the accelerator. For ATA  $\omega_0 Z_1 \approx .24 \text{ cm}^{-1}$  and  $L_g \approx 33 \text{ cm}$ . Use of Eq. (7) together with the measured noise level at the injector leads one to expect a final BBU amplitude of  $\approx 0.02 \text{ cm}$

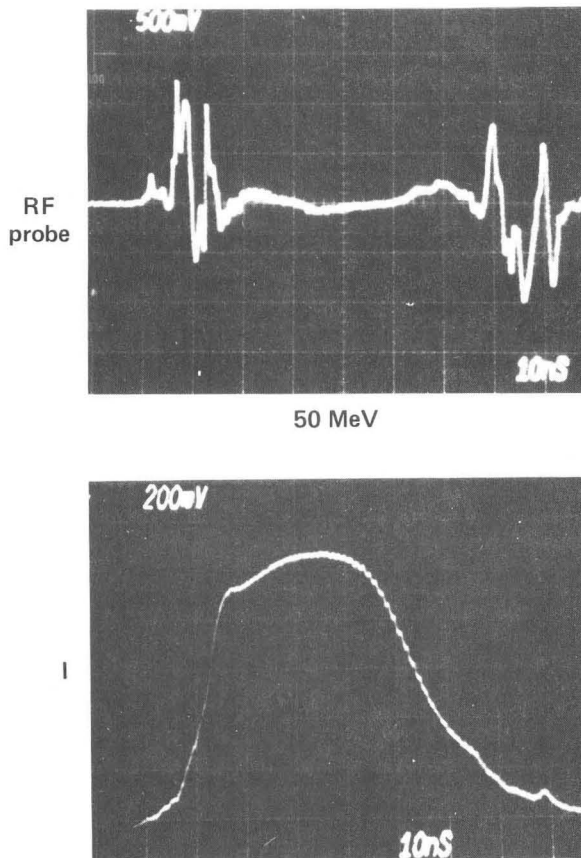


Fig. 10. Successful propagation of a 10 kA beam pulse down ATA. The entire charge survives passage through the accelerator and the  $B_{\theta}$  loop shows that the BBU amplitude is less than 0.01 cm.

due to the linear focusing of the channel for a 10 kA beam. Substitution into Eq. (14) or (15) indicates that total stability will be achieved if  $\epsilon > 0.01 I(\text{kA})$ . That is, for 10 kA  $\epsilon$  must be greater than 0.1 to stabilize the beam. Thus a 5% spread in  $k_{\beta}$  will stabilize 10 kA. It appears as though this level of nonlinearity has been achieved.

#### Summary

Optimal cavity design coupled with the proper magnetic transport system can greatly reduce BBU growth which is the primary obstacle to high current, high energy induction linac performance. Due to the phase mix damping provided by its non-linear focusing force laser ion-guiding can permit acceleration of high currents to arbitrarily high energies without BBU growth.

#### References

1. R. H. Helm, G. A. Loew and W.K.H. Panofsky, The Stanford Two-Mile Accelerator, R. B. Neal editor, New York: Benjamin, 1968, Ch. 6, pp. 203-237.
2. R. J. Briggs, "Suppression of Transverse Beam Breakup Modes in an Induction Accelerator by Gas Focusing," Univ: of CA. report UCID-18633, 1980.
3. V. K. Neil, L. S. Hall and R. K. Cooper, "Further Theoretical Studies of the Beam Breakup Instability," Part. Accel. 9, 213 (1979).
4. G. J. Caporaso and R. J. Briggs, to be published.

5. R. J. Briggs, D. L. Birx, G. J. Caporaso, V. K. Neil and T. C. Genoni, "Theoretical and Experimental Investigation of the Interaction Impedances and Q Values of the Accelerating Cells in the Advanced Test Accelerator," submitted to Particle Accelerators.
6. J. P. Reilly and K. L. Kompa, J. Chem. Phys. 73, 5468 (1980). See also W. E. Martin, G. J. Caporaso, W. M. Fawley, D. Prosnitz and A. G. Cole, "Electron-Beam Guiding and Phase-Mix Damping by a Laser-Ionized Channel," Phys. Rev. Lett. 54, 685 (1985) and references contained therein.

Work performed jointly under the auspices of the U.S. Department of Energy by the Lawrence Livermore National Laboratory under contract No. W-7405-ENG-48 and for the Department of Defense under DARPA, ARPA Order No. 4395 and 5316, monitored by Naval Surface Weapons Center under document number N60921-85-POW0001; SDIO/BMD-ATC MIPR #31-RPD-53-A127; and SDIO/NSWC reference number B00014-85-WR35514.